Characterization of a new *Klebsiella pneumoniae* amyloid in biofilm formation

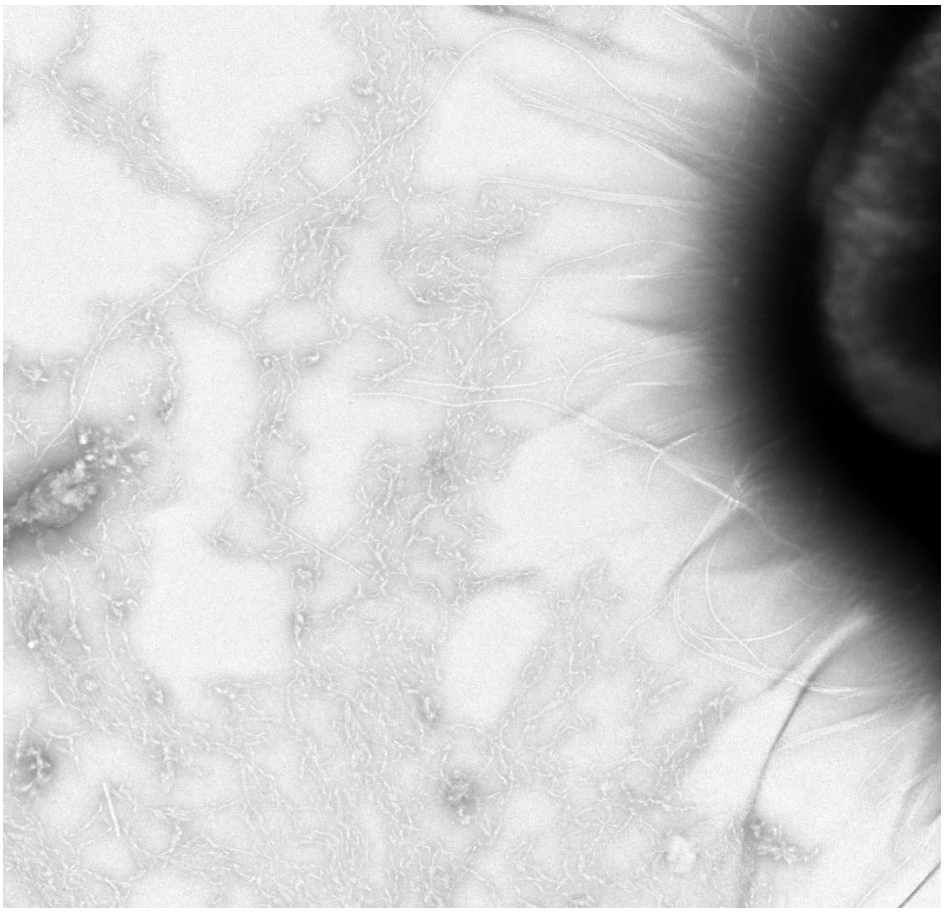

Master's thesis

Fatema Ali Moussa

Medicine with Industrial Specialization

Biomedicine

2022

AALBORG
UNIVERSITY

STUDENT REPORT

Project title:	Characterization of a new *Klebsielle pneumoniae* amyloid in biofilm formation
Project period:	September 2021 - May 2022
Semester:	Medicine with Industrial Specialization, Biomedicine, Master's thesis
ECTS:	60
Supervisor:	Svend Birkelund, Professor, Medical Microbiology and Immunology, Aalborg University
Co-supervisor:	Emil Kofod-Olsen, Lector, Medical Microbiology and Immunology, Aalborg University
Number of pages:	28

AALBORG UNIVERSITY

Department of Health Science and Technology, Aalborg University

Study Board of Medicine
Niels Jernes Vej 12, 5A
DK-9220 Aalborg Øst
Phone: 99402430
hn@hst.aau.dk

Abstract

The Gram-negative bacteria *Klebsiella pneumoniae* can cause severe infections in elderly, diabetics, and immunocompromised individuals, such as urinary tract infections (UTI), pneumoniae, and sepsis. Many UTIs are associated with indwelling urinary catheters since *K. pneumoniae* is able to colonize medical equipment; this is related to the fact that the pathogen is also able to create biofilms on catheters. The creation of biofilms on abiotic surfaces is also seen in other bacteria, such as *Escherichia coli*, from which it is known that amyloid fibers constitute most of the biofilm and it contributes to the formation of it. Amyloids in different bacteria have been identified, yet none have been characterized in *K. pneumoniae* strains. Thus, the aim of this study is to characterize a new *K. pneumoniae* amyloid in biofilm formation. To identify the amyloid, bacterial cultures with Congo red (CR) were made to create a biofilm. The biofilm was then assessed with brightfield- and fluorescence microscopy, and the fibers in this biofilm were characterized by electron microscopy (EM). Subsequent protein identification was performed by SDS-PAGE, in-gel digestion, MALDI-TOF MS and MS/MS. Of the seven *K. pneumoniae* isolates that were cultivated, isolate CA402 exhibited the most prominent results in biofilm formation, binding of CR and brightfield- and fluorescence microscopy, all displaying distinctive traits of amyloid fibers; CA402 was therefore used for the rest of the experiments. EM also displayed fibers with characteristic properties of amyloid, indicating these are amyloid fibers found in the biofilm. SDS-PAGE of the amyloid fibers that were treated with formic acid showed a distinctive band at 20kDa, indicating it could contain the amyloid protein. Four interesting peptide masses appeared after measuring with MALDI-TOF, but the peptide mass at 1510.738 m/z was the most distinctive. Subsequent MS and MS/MS revealed that this peptide matched with the MrkA subunit of type 3 fimbriae in a CA402 protein database. This indicates that the amyloid fiber found in *K. pneumoniae* CA402 is MrkA. The findings thereby provide a better understanding of the pathogenesis, as type 3 fimbriae are known to play a role in biofilm formation and MrkA is part of the type 3 fimbriae.

Resumé

Den Gramnegative bakterie *Klebsiella pneumoniae* kan give alvorlige infektioner i ældre, diabetikere og immunsupprimeret individer, såsom urinvejsinfektioner (UVI), lungebetændelse og sepsis. Mange UVI'er er associeret med indlagte urinkatetre, da *K. pneumoniae* er i stand til at kolonisere medicinsk udstyr; dette ses i forbindelse med at bakterien er i stand til at danne biofilm på katetre. Dannelsen af biofilm på abiotiske overflader ses også i andre bakterier som for eksempel *Escherichia coli*, hvorfra man ved at amyloide fibre udgør størstedelen af biofilmen og at den bidrager til dannelsen af det. Amyloider i forskellige bakterier er blevet identificeret, men alligevel er ingen blevet karakteriseret i *K. pneumoniae* stammer. Dermed er formålet med dette studie at karakterisere et nyt *K. pneumoniae* amyloid i forbindelse med biofilm formation. For at identificere amyloidet blev der lavet bakteriekulturer med Congo rødt (CR) for at danne en biofilm. Biofilmen blev derefter vurderet ved hjælp af lys- og fluorescence mikroskopi, og fibrene i biofilmen blev karakteriseret ved hjælp af elektronmikroskopi (EM). Efterfølgende blev proteinet identificeret ved udførelse af SDS-PAGE, in-gel digestion, MALDI-TOF MS og MS/MS. Ud fra de syv *K. pneumoniae* isolater der blev lavet bakteriekulturer af, udviste isolat CA402 de bedste resultater når det kom til dannelsen af biofilm, binding af CR og lys- og fluorescence mikroskopi; alle resultaterne viste særlige træk for amyloider. CA402 blev derfor brugt til resten af forsøgene. EM udviste også egenskaber karakteristiske for amyloid, hvilket tyder på at dette er amyloide fibre fundet i biofilmen. SDS-PAGE af de amyloide fibre, som blev behandlet med myresyre, viste et distinktivt bånd ved 20kDa, hvilket tydede på at dette kunne indeholde amyloid proteinet. Fire interessante peptid masser blev målt ved hjælp af MALDI-TOF, men peptidet ved 1510.738 m/z var det mest fremtrædende af dem. Efterfølgende viste MS og MS/MS at dette peptid matchede med MrkA subunit i type 3 fimbriae i en CA402 protein database. Dette tyder på, at det amyloide fiber fundet i *K. pneumoniae* CA402 er MrkA. Disse resultater giver en bedre forståelse af patogenesen, da type 3 fimbriae er kendt for at spille en rolle i biofilm formation og MrkA er en del af type 3 fimbria.

Abbreviations

A. actinomycetemcomitans = Aggregatibacter actinomycetemcomitans

c-di-GMP = Cyclic di-GMP

CR = Congo red

E. coli = Escherichia coli

EM = electron microscopy

FTIR = Fourier-transform infrared spectroscopy

GI = gastrointestinal tract

K. pneumoniae = Klebsiella pneumoniae

LB = Luria-Bertani

LPS = lipopolysaccharides

MALDI-TOF = matrix-assisted laser desorption/ionization time-of-flight

MS = mass spectrometry

MS/MS = tandem mass spectrometry

PBS = phosphate-buffer saline

PMF = peptide mass fingerprinting

SDS = sodium dodecyl sulfate

TEM = transmission electron microscopy

TFA = trifluoroacetic acid

ThT = Thioflavin T

UTI = urinary tract infection

Table of contents

Introduction

Klebsiella pneumoniae is a Gram-negative bacterium, part of the Enterobacteriaceae family, and as an opportunistic pathogen it is the cause of many severe infections in mostly immunocompromised individuals, diabetics, and elderly. It usually causes urinary tract infections (UTIs), pneumonia, liver abscess, bacteremia, and sepsis, of which the mortality rates of the latter have increased due to fewer choices of treatment caused by the multi-drug resistant nature of the pathogen ***(1, 2)***. *K. pneumoniae* is found in the environment, like in water and soil, but can also colonize medical equipment, such as urinary catheters and endotracheal tubes. The pathogen can also be found in the mouth, pharynx, or the gastrointestinal tract (GI), which are all places it resides and colonizes without necessarily causing an infection ***(1, 3)***. However, from here, the bacterium can infect its host by spreading to other parts of the body ***(1)***. About 5% of *K. pneumoniae* infections in hospitalized patients were associated with colonization of the GI prior to admission, as it was discovered that the strains from the infection and colonization were mostly the same ***(4)***. Colonization of the GI with *K. pneumoniae* is thought to induce most of the UTIs that are caused by the pathogen; however, these infections can also be due to the insertion of urethral catheters, since medical devices can work as an entrance for pathogens ***(1)***. In addition, *K. pneumoniae* can create a biofilm on the catheters; the creation of this biofilm is usually seen in relation to UTIs caused by the bacteria, thus factors leading to the formation of biofilm probably play an essential part in the pathogenesis ***(1, 3, 5)***.

Klebsiella pneumoniae and its pathogenesis

K. pneumoniae is a rod-shaped and non-motile bacterium that has a capsule consisting of polysaccharides surrounding its outer membrane (fig. 1). The most important virulence factors of *K. pneumoniae* are the capsule, lipopolysaccharides (LPS) and pili, also known as fimbriae, protruding from the surface of the pathogen ***(1, 4)***. The capsule is an important virulence factor, as it serves in protecting the bacteria from the immune system by inhibiting phagocytosis and opsonization by e.g., macrophages and neutrophil granulocytes ***(3, 4)***. Several capsular serotypes (total of 78) have been identified based on strain-specific polysaccharides ***(1, 3)***. However, two of these serotypes, K1 and K2, are more virulent than the other serotypes and are usually found in the hypervirulent strains ***(1)***. Additionally, K1 and K2 hypervirulent strains are mostly found in Asian countries ***(6)***. The capsule in the hypervirulent strain is found to be much larger due to the enhanced production of polysaccharides; the thicker capsule leads to even more resistance towards phagocytosis and other defense mechanisms ***(1, 7)***. The hypervirulent strain is therefore exceedingly invasive, making it able

to infect both healthy and immunocompromised individuals ***(1, 3, 7)***. In contrast to the hypervirulent strain, the classical strain of *K. pneumoniae* is less virulent and usually causes serious infections in elderly and immunocompromised individuals ***(1, 7)***. Over time, these classical strains have obtained antibiotic-resistance due to the acquisition of plasmids containing resistance genes, or mutations in the genome ***(4, 6)***. All *K. pneumoniae* strains can express β-lactamases resulting in ampicillin resistance, whereas extended-spectrum β-lactamases are common and carbapenemases are rear in Danish isolates, which reduces the treatment options available for these kinds of infections, making the mortality and morbidity rates higher ***(1, 4, 8, 9)***. The virulence factor LPS consists of three components being the O antigen, the core oligosaccharide and lipid A, which is embedded into the outer membrane ***(3)***. It protects the bacteria from the humoral response of the immune system, including increased resistance towards complement killing ***(1, 3)***. However, it can also activate a cellular response as lipid A is recognized as a ligand by a pattern recognition receptor ***(1)***.

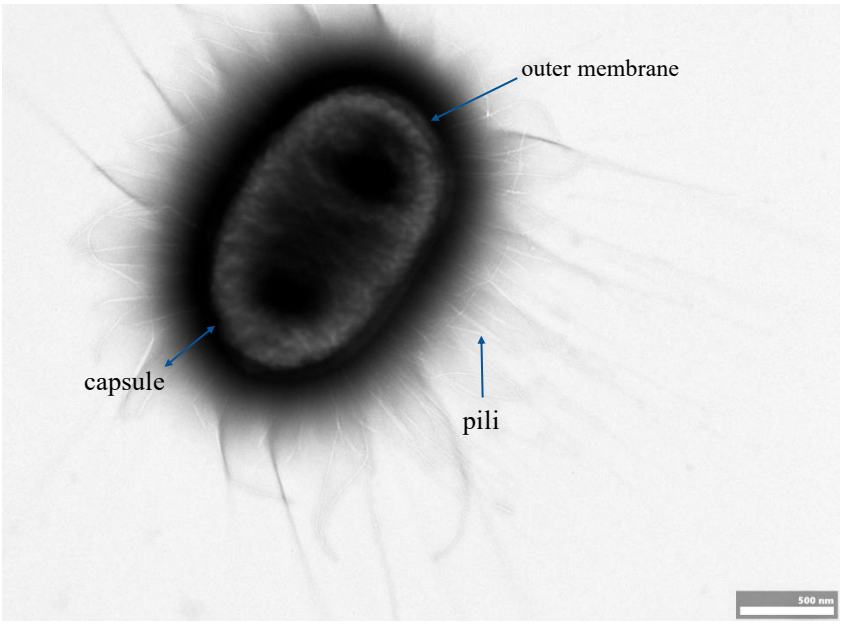

Figure 1: An electron micrograph of a Klebsiella pneumonia isolate CA402. The picture illustrates its rod-shape, and the arrows point towards its outer membrane, capsule, and pili (also known as fimbriae).

Lastly, the pili of *K. pneumoniae* is also an important virulence factor that plays a part in adherence to surfaces, both biotic and abiotic ***(1, 3)***. A few types of fimbriae have been identified, such as Kpc fimbriae, KPF-28 adhesin, type 1 fimbriae and type 3 fimbriae ***(1, 3)***. Most of the adhesins that are involved in the urinary tract, and the colonization of it, are type 1 and type 3 fimbriae, which are the most investigated and characterized, in contrast to Kpc fimbriae and KPF-28 adhesin ***(1, 5)***. Type 1

fimbriae are characterized as long, thin, and filamentous structures extending from the outer membrane and beyond the capsule, while type 3 usually are 0.5-2µm in length and 2-4nm wide and have a helical structure supported by β-strands ***(1, 3, 10)***. *K. pneumoniae* has several gene clusters possibly encoding its fimbrial antigens, and type 1 and 3 fimbriae are each constituted by their own gene cluster ***(3, 5)***. Type 1 has the *fimBEAICDFGHK* gene cluster; most of the structure in type 1 is comprised of FimA subunits (encoded by *fimA),* whereas FimH (encoded by *fimH*) is located at the outer end, forming the adhesive component. The rest of the genes encode subunits that are minor structures and proteins responsible for the assembly of the fimbrial structure ***(1, 3)***. Due to the *fim* gene cluster, type 1 fimbriae can bind to soluble mannose or cells with structures containing mannose, making it mannose-sensitive ***(3, 5)***. Type 1 fimbriae are also found in other *Enterobacteriaceae*, though the gene sequence differs from pathogen to pathogen ***(5)***. The gene expression of the *fim* cluster is regulated by *fimS*, an invertible DNA component, which works as the promoter region of the operon; meaning if it is not "on", transcription will not take place ***(3, 5)***. Type 3 has the gene cluster *mrkABCDF*, where the MrkA subunit constitutes the majority of the fimbrial structure, MrkD is the subunit with the adhesive properties based at the edge, and MrkB, -C and -F are the proteins responsible for assembling the structure and stabilizing it ***(1, 3)***. The MrkA subunit encompasses the aforementioned β-strands, that contribute to the helical structure of the fimbria, which are located in its C-terminal region ***(5, 10)***. In contrast to type 1, the adhesin MrkD is not able to bind mannose, making type 3 fimbriae mannose insensitive. Though a definite binding site of MrkD has not yet been fully elucidated, it has been found to bind collagen proteins ***(1, 5, 10)***. Binding to biotic surfaces is facilitated by MrkD, but when it comes to adhesion on an abiotic surface, such as urinary catheters, MrkA is responsible ***(5)***. The regulation of *mrk* operon expression is managed by MrkJ, -H and -I, all encoded by three genes located adjacent to *mrkABCDF* ***(5, 10)***. Basically, they are able to sense and affect cyclic di-GMP (c-di-GMP) concentrations in the pathogen; when the change in concentration levels has been recognized, c-di-GMP is then bound to an effector molecule containing a domain, which is subsequently enabled to regulate different processes. Thus, with the *mrkHIJ* being close to the *mrkABCDF* cluster, it is able to regulate the expression of *mrkABCDF* when c-di-GMP levels are adjusted; several studies support these findings of *mrkHIJ* regulating the expression of type 3 fimbriae ***(10-13)***. Both type 1 and type 3 fimbriae play a role in adhesion to cell surfaces, like the epithelial cells in the bladder, contributing to UTIs, but only type 3 is important in biofilm formation as it is expressed during the process ***(1, 4)***. Some studies suggest that type 1 also plays a part in biofilm formation, yet it is not entirely clear ***(1, 5)***.

Biofilm formation

In order for *K. pneumoniae* to grow, it has several virulence factors that play a role in protecting it from immune responses of the infected host, and thereby are a part of its pathogenesis; one of these factors is the biofilm formation ***(1, 5)***. A biofilm is defined as a community of bacteria that are bound to a surface and supported by an extracellular matrix that is created by the bacteria itself ***(14, 15)***. When a surface area comes into contact with free-living bacteria, a biofilm can be formed on it as the bacteria adhere to it ***(1)***. The process itself is more complicated, but after the initial attachment, it involves the formation of microcolonies, mature biofilm formation, and eventually releasing free-living bacteria ***(5, 10)***. These planktonic bacteria can then go on to colonize and infect the host ***(1)***. *K. pneumoniae* biofilm formation is usually associated with indwelling medical devices such as urinary catheters, and therefore suggested to be associated with nosocomial infections like catheter associated UTIs ***(3, 5, 10)***. It is also proposed that type 3 fimbriae are associated with UTIs, since they are involved with biofilm formation ***(1, 3)***. Adherence to the surface of the catheters is facilitated by type 3 fimbriae; specifically, MrkA binds to the abiotic surface without requirement of the adhesive MrkD, making MrkA essential for the formation of biofilm. However, after insertion of a device, proteins and cells derived from the host will coat it, meaning MrkD could possibly mediate the biofilm formation ***(1, 5, 10)***. Overall, type 3 fimbria has been found to be necessary for biofilm formation, as studies have shown that *K. pneumoniae* strains that only expressed type 1 fimbriae were restricted in binding to biotic surfaces, and therefore no biofilm was formed ***(10)***.

The matrix created by the biofilm is composed of several components such as DNA, polysaccharides, and proteins, all generated from the pathogen ***(5, 14)***. The role of the biofilm is to protect the pathogen; the dense matrix acts as a barrier to the surrounding environment as it ensures endurance against antibiotics and defense mechanisms coming from the host ***(3, 14, 15)***. The bacteria in the matrix are highly protected, since antimicrobials have a difficulty in reaching them, but also because their antibiotic resistance is increased ***(1, 5, 15)***. The bacteria embedded inside the matrix grow more slowly compared to free-living bacteria, making them less susceptible to antibiotics targeting bacteria that are actively dividing ***(5, 14)***. Additionally, alterations in the gene expression of these bacteria in comparison to planktonic bacteria, gives rise to further antibiotic resistance. Furthermore, these genetic changes can easily be transferred between the bacteria, since this mechanism is improved in a biofilm ***(5, 10)***. One of the proteins in the biofilm is functional amyloids, which comprise the majority of the matrix ***(15)***. Amyloid fibers are highly aggregated proteins consisting of β-strands that are helically packed perpendicularly to the axis of the fiber, giving them a unique cross-β pattern;

amyloids are morphologically filamentous and not branched, with a diameter and length approx. 2-20nm ***(15, 16)***. The structure of amyloid fibers has been enlightened by the use of electron microscopy (EM) ***(17)***. Furthermore, these β-sheets are defined by an x-ray diffraction pattern with a reflection at approx. 4.8Å and 10Å, by using electron paramagnetic resonance profiles or Fourier-transform infrared spectroscopy (FTIR) ***(15-17)***. Moreover, amyloids are highly resistant to denaturation by chemicals such as sodium dodecyl sulfate (SDS) and high temperatures, as well as proteolysis by protease K, due to the highly aggregated form of the fibers ***(15, 18, 19)***. To dissolve amyloid fibers, formic acid in very high concentrations (>70%) is required ***(15, 18)***. Amyloids have also shown to have tinctorial characteristics, meaning they can be detected with coloring using the dyes Thioflavin T (ThT) and Congo red (CR), as the cross-β backbone of the fibers is able to bind to these dyes ***(15, 17, 18)***. Binding to ThT and CR results in an enhanced fluorescence and a red shift in light, respectively, when the dyed amyloid is examined with microscopy ***(15, 17, 19)***. However, these dyes are not definite indicators of amyloid, as they are both able to bind to other proteins than amyloid, and CR is also able to bind cellulose ***(15, 16)***. Some of the well-known amyloids in bacteria are: curli fibers created by *Escherichia coli* (*E. coli*) and *Salmonella*, Fap by *Pseudomonas*, TasA by *Bacillus subtilis*, and Bap and PSM by *Staphylococcus* ***(15, 18)***. The most well defined of these amyloids are curli in *E. coli* ***(18)***. The curli fibers are short, thin, and very coiled in appearance; from studies about biofilm formation in *E. coli*, it is known that curli supports the matrix biofilm by giving it structure and adherence, and thereby contributing to its formation ***(15, 19)***. Overall, amyloids are found to be associated with biofilm formation, which contributes to endurance and colonization, and thereby bacterial amyloids contribute indirectly to the pathogenesis of the bacteria ***(15)***.

Aim of study

K. pneumoniae has been found to reside on equipment such as urinary catheters, by creating a biofilm helping the bacteria adhere to its surface. The majority of the biofilm is comprised of amyloid fibers, which also play a part in forming it. Most bacterial amyloid studies that have been conducted are about *E. coli* and their curli amyloids, but none has been found in the literature about the amyloid fibers in *K. pneumoniae*. To understand the pathogenesis of *K. pneumoniae* better, it would be interesting to investigate what causes the biofilm formation, and thereby identify the amyloid fiber that contributes to this formation. Hence, the purpose of this study is to characterize a new *K. pneumoniae* amyloid in biofilm formation.

Materials and methods

K. pneumoniae isolates

The following seven clinical *K. pneumoniae* blood or urine isolates (Department of Clinical Microbiology, Aalborg University Hospital, Denmark) were used: KPN391, CA402, UTI3104, UTI4409, UTI4741, UTI5245 and UTI5829.

Bacterial cultures and biofilm formation

To replicate the biofilm *K. pneumonia* creates on catheters and other medical tubes, overnight cultures of the seven isolates were cultivated in each their flask with Luria-Bertani (LB) medium (Sigma-Aldrich, St. Louis, MO, USA) with 3% CR stain (Sigma-Aldrich, Germany) and incubated at 30°C for 18 hours with shaking at 90 rpm. Subsequently, the flasks were examined for biofilm formation and pictures of the flasks were taken. Cultures in beakers were also made and a lid was put on top of it. Glass slides were hanging from the lid and submerged halfway into the liquid, in order for the biofilm to be formed on the glass slides when shaking overnight in the incubator. This gave access to assess the biofilm for microscopy, and for more experiments to be conducted.

Brightfield- and fluorescence microscopy

An amount of 40µl from the bacterial cultures was added to a glass slide and pictures were taken of each isolate using the automated Leica DM5500B research microscope (Leica Microsystems, Wetzlar Germany) with a Jenoptik Gryphax microscope camera and the associated Gryphax software (Jenoptik, Jena, Germany). Pictures were also taken of the biofilm formed on the glass slides during cultures overnight. To examine the possible biofilm formation, the samples were assessed using the brightfield function of the microscope, as well as the fluorescence function with the I2 filter. Pictures were taken using the 40X objective.

Transmission electron microscopy (TEM)

TEM was performed according to Jensen et al. ***(2)***. A CA402 bacterial culture in LB medium had been incubated over night, after which a five µl sample was taken for EM. The aliquot was added to a 400-mesh glow-discharged nickel grid with a carbon coat for one minute, after which it was washed with phosphate-buffered saline (PBS). A drop of 1% phosphotugenic acid was added to stain the sample and then blotted dry on filter paper. TEM was performed on a JEM-1400 electron microscope

(JEOL, Tokyo, Japan) at 60keV connected to an electron-sensitive CCD camera (TVIPS digital camera, Gauting, Germany).

SDS-PAGE

The biofilm on the glass slides was scraped off and suspended in 300µl Milli-Q water in an Eppendorf tube and centrifuged at 10.000 x g for 10 minutes at 20°C, whereafter the supernatant was removed, and the pellet resuspended in 200µl Milli-Q water. The tube was centrifuged twice and the pellet resuspended in 200µl Milli-Q water both times. To completely purify the amyloid from the bacteria, the sample was freeze-dried. A small hole was made on the lid of two new Eppendorf tubes and 25µl of the sample was distributed into each of them; 25µl Milli-Q water was added to one of the tubes, while 25µl formic acid (ThermoFisher, Waltham, MA, USA) was added to the other tube. The samples were then dried by freezing in a high vacuum for 2 hours. After being freeze-dried, 50µl SDS loading buffer (75mM Tris at pH 8, 0.6% SDS, 15% glycerol, 8M Urea, 0.9mg Bromophenol blue) was added to each tube and mixed well before transferring the content of the tubes into new Eppendorf tubes. Subsequently, the samples were prepared for SDS-PAGE; 10µl sample buffer (2x Laemmli sample buffer, 2-Mercaptoethanol) was added to each tube which were then put in a heating block for 10 minutes at 100°C. Ten µl of each sample was loaded in a Mini-PROTEAN TGX precast gel (Bio-rad, California, USA); for the ladder, 10µl PageRuler Unstained Broad Range Protein Ladder (ThermoFisher, Waltham, MA, USA) was used. The SDS-PAGE was run for approx. 30 minutes or until the bands were almost at the bottom of the gel. Thereafter, the gel was stained at room temperature for 30 minutes with agitation, using 50ml Coomassie blue stain (Coomassie blue stain, acetic acid, Milli-Q water). The Coomassie solution was then removed and destain (30% methanol and 10% glacial acetic acid) was added until it covered the gel; a little sponge was added to the corner of the box containing the gel and destain. The gel was destained over night with agitation. The next day, pictures of the gel were taken using the EPSON Perfection 4490 scanner and Epson scan software (Epson, Suwa, Nagano, Japan).

In-gel digestion and protein purification

In-gel digestion was performed according to Shevchenko et al. ***(20)*** with minor modifications. Firstly, the destain was removed from the gel and distilled water was added to the box that the gel was kept in. The gel was stored in the distilled water for approx. 30 minutes with agitation, the water being changed after the first 15 minutes. Thereafter, the bands of interest were cut out of the gel using a scalpel and then cut into small cubes (1x1mm) and put into microcentrifuge tubes for each sample.

Firstly, 500µl acetonitrile was added and the tubes were incubated at room temperature for 10 minutes or until they gel pieces shrink. After removing the acetonitrile, 100µl of a triethylammonium buffer (100mM triethylammonium bicarbonate, tris-(2-carboxyethyl)-phosphine hydroxychlorid) was added to the tubes, which were then incubated for 30 minutes at room temperature with shaking. The buffer was removed and 500µl acetonitrile was added and removed after 10 minutes, after which an alkylating buffer (chloroacetamide, 100mM triethylammonium bicarbonate) was added, and the tubes were incubated for 20 minutes in the dark at room temperature. After removing the buffer, acetonitrile was added one last time and after removing it, 50µl of a trypsin buffer (trypsin protease (dissolved in distilled water), acetonitrile, 10mM triethylammonium bicarbonate) was added and the tubes were incubated at 37°C overnight.

MALDI-TOF mass spectrometry, Peptide Mass Fingerprinting (PMF)

Preparations for matrix-assisted laser desorption/ionization time-of-flight (MALDI-TOF) mass spectrometry (MS) was performed according to Shevchenko et al. ***(20)*** with minor modifications. After the gel pieces had been trypsin treated overnight, the tubes were cooled down to room temperature and thereafter centrifuged (500 x g, 10 minutes, 20°C) to spin down the gel pieces. Next, the digest of the tubes was transferred to new tubes, while the tubes containing the gel pieces were washed and filled with distilled water; the gel pieces were stored at -20°C. Aliquots of the digest could now be used for protein identification using MALDI-TOF. Firstly, a MALDI matrix was made using α-cyano-4-hydroxycinnamic acid dissolved in a buffer (acetonitrile, distilled water, trifluoroacetic acid (TFA) 1.25%). Subsequently, droplets (0.75µl) of the digests were loaded on to a Maldi target plate, after which droplets of the matrix were loaded on top of the samples. The droplets were then left to dry on the target plate before continuing. Peptide mass fingerprinting (PMF) was measured by MALDI-TOF using the ultrafleXtreme MALDI-TOF mass spectrometer (Bruker, MA, USA). The peptide masses were measured and analyzed with the flexControl, flexAnalysis and BioTools software (Bruker, MA, USA). Data was compared with a translated *K. pneumoniae* CA402 genome database, and the result from the database was compared in a protein database using the protein BLAST program (NCBI, MD, USA).

Results

Biofilm characterization

In this study, bacterial cultures of seven *K. pneumoniae* isolates were made in flasks and incubated at 30°C with shaking in order to promote the formation of a biofilm (fig. 2). As seen in figure 2, five of the isolates produced a clear red line on the side of the flasks (fig. 2A, C, D, F, G), while two of them did not (fig. 2B, E). Compared to isolates UVI3104, UVI4409, UVI5245 and UVI5829 (fig. 2C, D, F, G), the CA402 isolate (fig. 2A) had a more clear and visible bright red line formed at the side of the flask at the air-liquid interface.

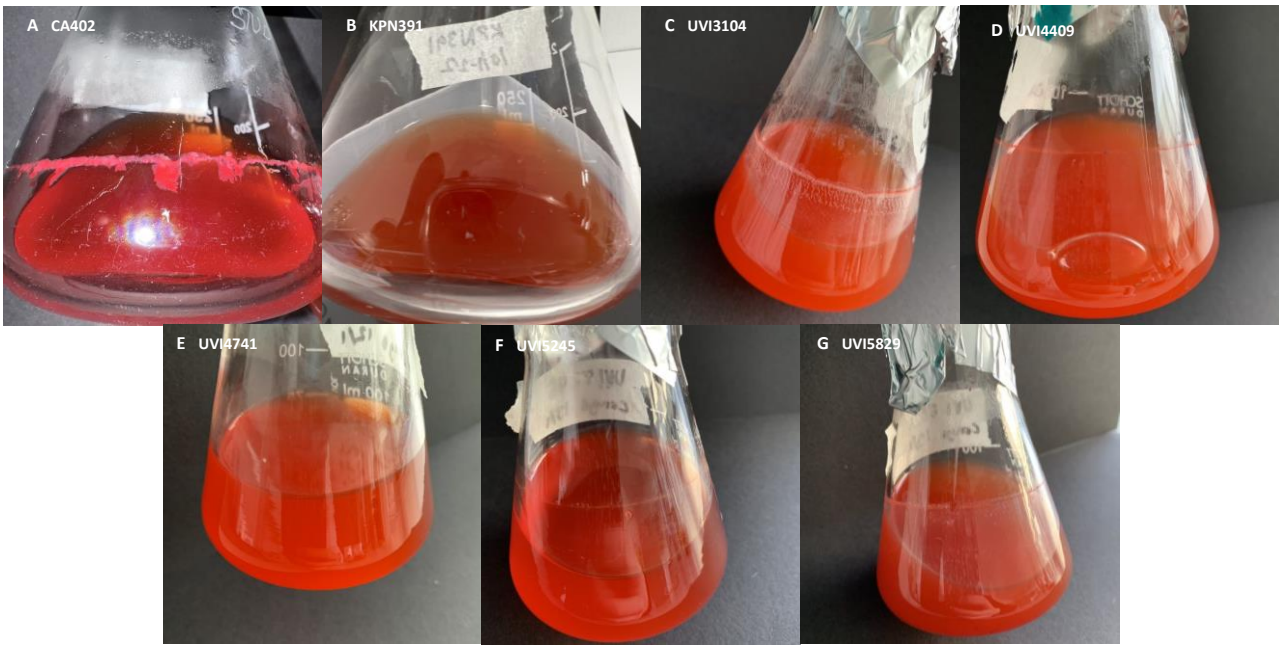

Figure 2: Flasks with bacterial cultures made with LB medium and containing Congo red. The cultures had been incubated overnight with shaking at 30°C. As seen in pictures A, C, D, F and G, a red line was formed on the side of the flasks, but more visible in figure A containing the K. pneumoniae isolate CA402. In pictures B and E, no red line was formed. A) CA402, B) KPN391, C) UVI3104, D) UVI4409, E) UVI4741, F) UVI5245, G) UVI5829. LB = Luria-Bertani.

To evaluate the biofilm that was formed on the flasks, bacterial cultures in beakers were also made, with glass slides hanging from a lid, submerging halfway into the cultures. Pictures were then taken of the biofilm that was formed on the glass slides or samples from the cultures were added to a glass slide. Pictures were obtained using the brightfield- and fluorescence microscope (fig. 3). Illustrated in figures 3A and 3B, is the biofilm that was formed on a glass slide by isolate CA402. The picture shows an abundance of red colored threadlike fibers with bacteria surrounding it (fig. 3A). The picture from the fluorescence microscope illustrates the same fibers but fluorescing in a red-orangey hue due

to the CR stain that shifts the light towards red, when binding to amyloid (fig. 3B). The isolates KPN391, UVI4409 and UVI4741 (fig. 3C, G, I) showed a few red spots on the brightfield images, but not visible fibers like in isolate CA402 (fig. 3A). The fluorescence, however, made it a bit clearer

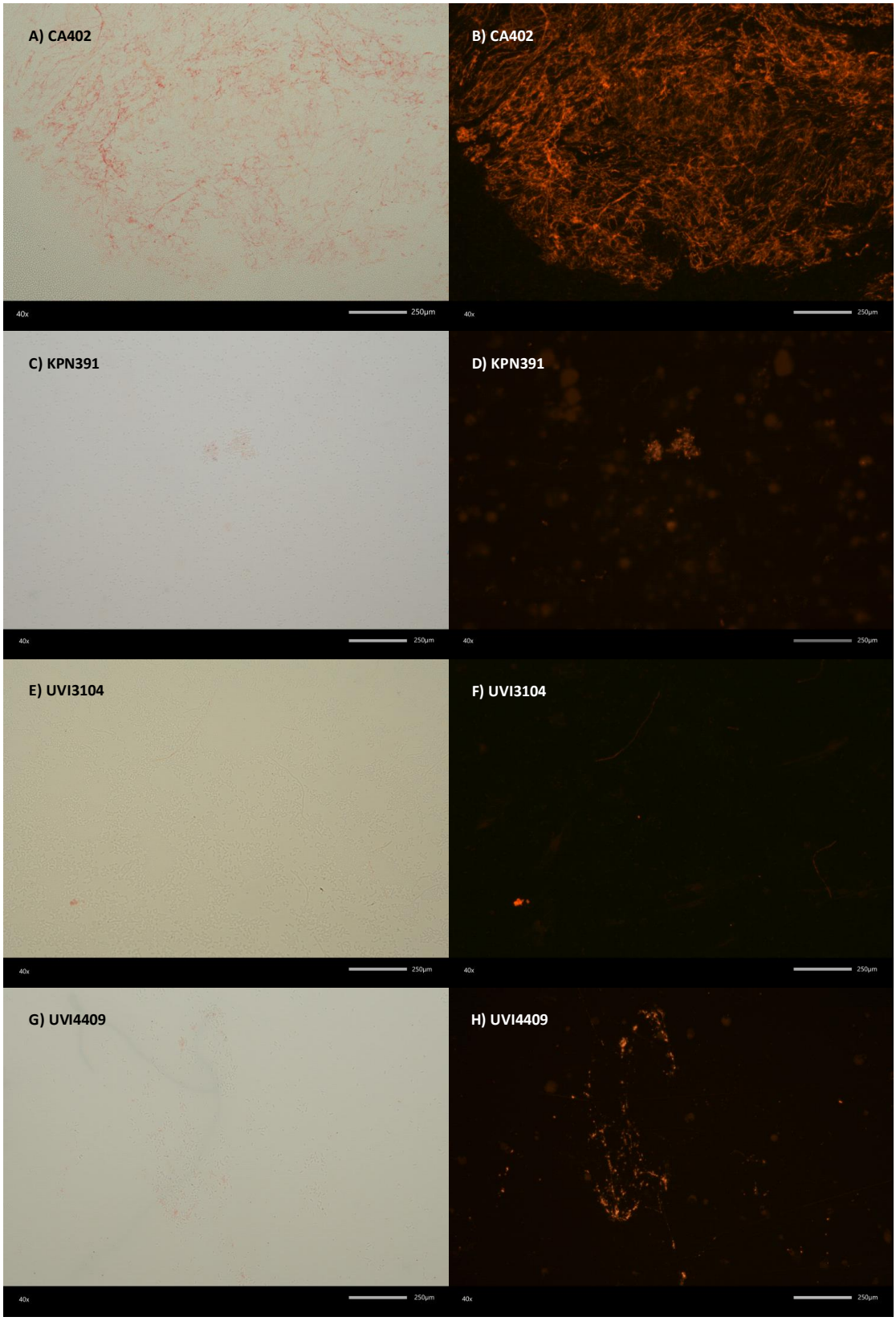

Figure 3: Brightfield- and fluorescence microscopy pictures of the biofilm formed by the different isolates on either a glass slide or a sample of the bacterial culture added to a glass slide. A-B) CA402, C-D) KPN391, E-F) UVI3104, G-H) UVI4409, I-J) UVI4741, K-L) UVI5245, M-N) UVI5829.

to what had bound to the CR, yet it did not look like clear fibers (fig. 3D, H, J) as with isolate CA402 (fig. 3B). In contrast, isolates UVI3104, UVI5245 and UVI5829 (figure 3E, F, K, L, M, N) displayed very little color in both the brightfield and fluorescence pictures, indicating almost no sign of amyloid fibers in the cultures.

Analysis of fibers formed by CA402

CR stain is known to dye amyloid fibers, and since the isolate CA402 appeared to have the most prominent results of biofilm formation and the microscopy results of it depicted the best picture of amyloid compared to the other isolates, we decided to continue the experiments with only CA402 going forward. To further investigate the possible amyloid CA402 creates, EM was used. Illustrated in figure 4 are electron micrographs taken of the biofilm generated by CA402. In the background, what seems to be amyloid fibers are seen surrounding the bacteria (oval structures of approx. 1µm, fig. 4A). Looking at a close-up view, the fibers are pictured as long but aggregated filaments (fig. 4C, D), and reaching out of the bacteria and its capsule are the pili, pictured as thin and long strands

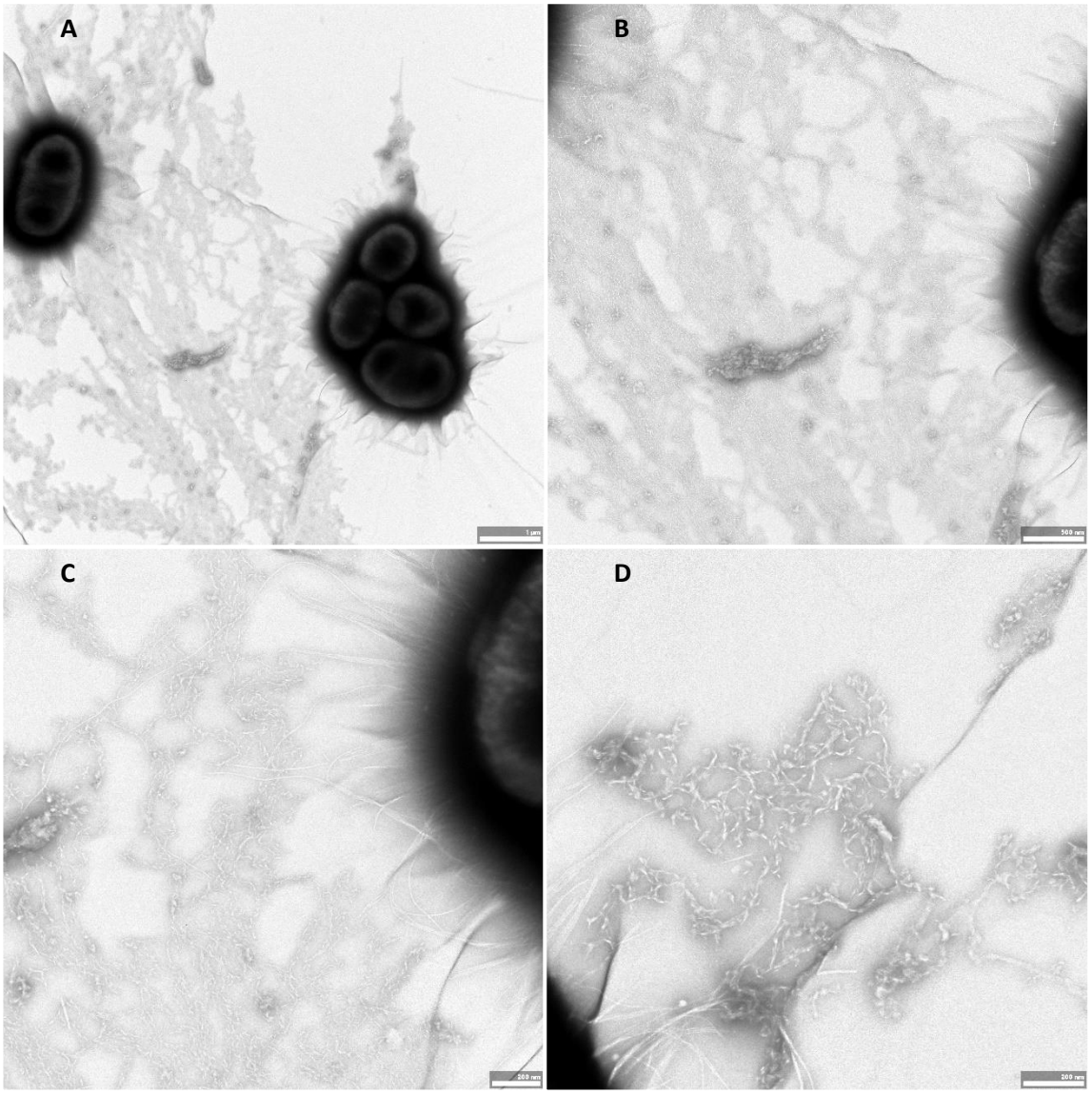

Figure 4: TEM of the biofilm formed by the isolate CA402. A) Fibers and bacteria in the biofilm are pictured, image taken with 5000x magnification. B-D) Close up view of the aggregated filaments, as well as the pili reaching out from the bacteria, each picture taken with 10.000x, 20.000x and 25.000x magnification, respectively. TEM = transmission electron microscopy.

reaching out to the filaments in the surrounding environment (fig. 4B, C). Thus, taking the preceding findings in to consideration, the fibers ability to bind CR and the morphological characteristics of the filaments illustrated in the electron micrographs, all indicate that these are amyloid fibers found in the biofilm.

Protein identification

In this study, SDS-PAGE was run to purify the amyloid protein that may constitute the formation of biofilm. The biofilm that was formed on glass slides was collected, treated with formic acid, and freeze-dried, to subsequently be loaded on to an SDS-gel. Formic acid was used since very low pH levels are needed to dissolve amyloid fibers, and high concentrations of formic acid is known to dissociate the fibers. As seen in figure 5A, the sample treated with formic acid showed a distinctive band at 20kDa that was not seen in the sample with water, indicating this band could contain the

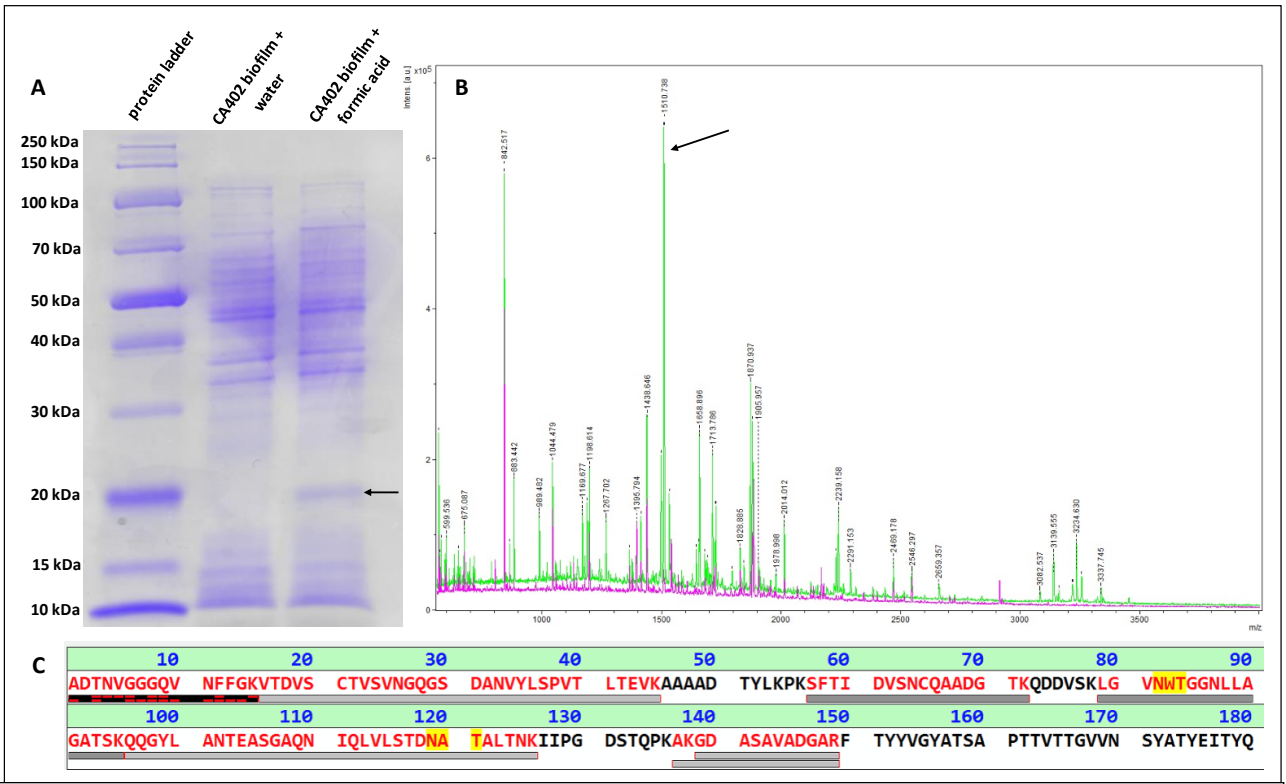

Figure 5: A) SDS-page gel of the protein purified from the CA402 biofilm, stained with Coomassie blue. Prior to running the SDS-page, each sample was either treated with water or formic acid while freeze-drying. A distinct band around 20 kDa (marked with an arrow) from the formic acid sample was shown compared to the sample with water. The bands at 20 kDa were cut out and in-gel digested for MS. B) Results of MS that was run on the digested proteins from the sample treated with water (purple peaks) and the sample treated with formic acid (green peaks). When comparing the two spectrums, there is a definite green peak that differs from the purple spectrum at 1510.738 m/z (marked with an arrow), indicating this is the purified protein of interest. C) The peptide at 1510.738 m/z was further fragmented and MS/MS was run, resulting in a peptide sequence that was compared in the CA402 protein database. The peptide sequence found by MS/MS matched with the known peptide sequence of MrkA in the database. The matching sequence is illustrated as a grey bar under the sequence from the database (the match is marked with red letters). The red bricks inside the black bar are the matching MS/MS information. SDS-PAGE = sodium dodecyl sulfate-polyacrylamide gel electrophoresis, MS = mass spectrometry, MS/MS = tandem mass spectrometry

amyloid protein. To identify the protein of interest, the bands at 20kDa were cut out of the gel and the proteins were trypsin treated over night, after which MS was performed using MALDI-TOF. When the laser hit the target plate containing the digested protein and MALDI matrix, a peak representing the mass-to-charge ratio (m/z) of each peptide it measured, appeared in a spectrum (fig. 5B). The peptides were measured a few times until a satisfactory sum of spectra was obtained. The peaks in the spectra of each of the two samples were then automatically assigned masses. The spectrums were then combined in order to compare the peaks as illustrated in figure 5B. The digested proteins that were treated with formic acid are the green peaks, while the purple peaks are the digested proteins from the sample that was treated with water. There are four interesting green peaks at 1510.783 m/z, 1713.786 m/z, 1870.937 m/z and 2239.158 m/z, which are different from the purple peaks, indicating one of these is our protein of interest (fig. 5B). The peaks at 1713.786 m/z, 1870.937 m/z and 2239.158 m/z were all analyzed through PMF and further fragmented and analyzed, but they did not match with any protein sequence. The peak at 1510.738 m/z seemed to be more distinct from the sample control compared to the three other peaks, and by the means of PMF, the protein was identified as MrkA. To specify the identification of our protein, the peptide was further fragmented with the laser, obtaining small ions that were then measured and tandem mass spectrometry (MS/MS) was thereafter performed. The results from the MS/MS were then run in a protein database for CA402. The open reading frames in the genome of CA402 were previously translated into protein sequences by using EMBOSS software, after which these protein sequences were assembled into a protein database for CA402, meaning our fragments are compared at the levels of amino acids. The results from the MS/MS were matched with some of the MrkA protein in the database, but not with a great score. The protein sequence from the database that matched (fig. 6A) was put into a peptide prediction program, SignalP 5.0 (DTU Health Tech, Kgs. Lyngby, Denmark), to predict the signal peptide cleavage site of this protein sequence (fig. 6B). With this information, we removed the leading strand up to the peptide according to the cleavage point (fig. 6B) and inserted the new and more precise sequence of the predicted peptide into the CA402 database (fig. 6C), while still keeping the original protein sequence in the database. MS/MS was then run again, and the data compared in the database, this time resulted in a better match. The fragmented sequence aligned better with the new MrkA peptide sequence within the database this time, giving us a stronger match between the peptide sequence found by MS and the known peptide sequence of MrkA (fig. 5C). When using the protein BLAST program (NCBI, MD, USA) to search in the database for the predicted peptide sequence from the MrkA protein sequence, a match is found with the type 3 fimbria major subunit of the MrkA

protein in *K. pneumoniae*. These results indicate that the type 3 fimbria major subunit MrkA is the amyloid protein that has been purified from the biofilm that was formed.

A

>MrkA__CA402 lib369410_6623_2_1_(paired)_contig_14_1165 [271658 - 271047] (REVERSE SENSE)
MAMKKVLLSAAMATAFFGMTAAHAADTNVGGGQVNFFGKVTDVSCTVSVNGQGSDANVYL
SPVTLTEVKAAAADTYLKPKSFTIDVSNCQAADGTKQDDVSKLGVNWTGGNLLAGATSKQ
QGYLANTEASGAQNIQLVLSTDNATALTNKIIPGDSTQPKAKGDASAVADGARFTYYVGY
ATSAPTTVTTGVVNSYATYEITYQ

B

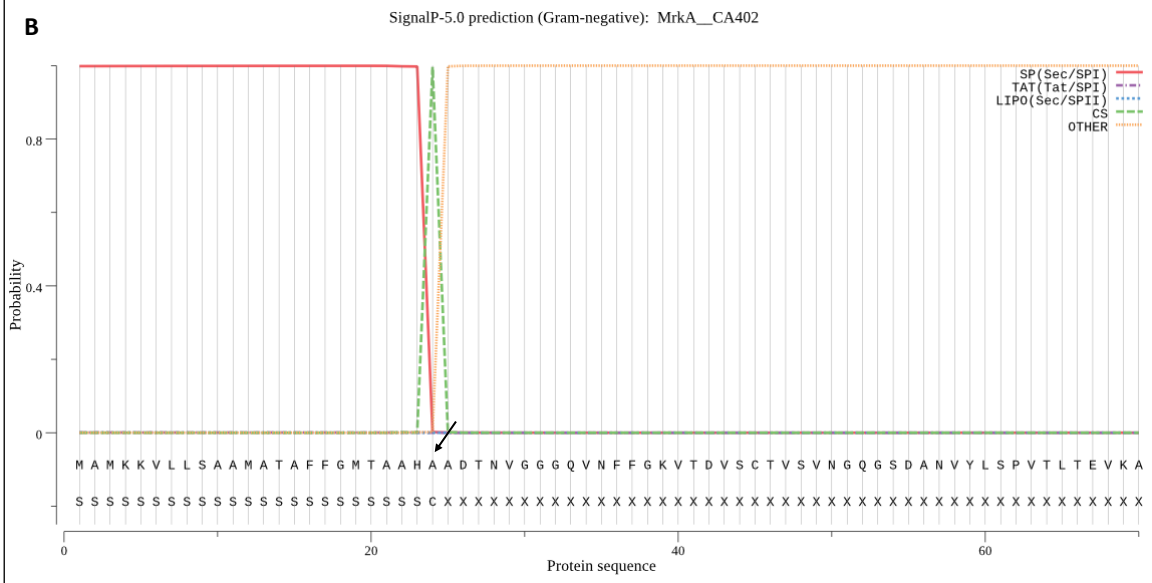

C

>MrkA_CA402_signalP lib369410_6623_2_1_(paired)_contig_14_1165 [271658 - 271047] (REVERSE SENSE)
ADTNVGGGQVNFFGKVTDVSCTVSVNGQGSDANVYL
SPVTLTEVKAAAADTYLKPKSFTIDVSNCQAADGTKQDDVSKLGVNWTGGNLLAGATSKQ
QGYLANTEASGAQNIQLVLSTDNATALTNKIIPGDSTQPKAKGDASAVADGARFTYYVGY
ATSAPTTVTTGVVNSYATYEITYQ

Figure 6: A) The MrkA protein sequence from the K. pneumoniae CA402 database. B) The predicted peptide an its cleavage site is pictured here, the arrow indicating cleavage point where the leading strand up to the peptide was deleted. The program SignalP 5.0 (DTU Health Tech, Kgs. Lyngby, Denmark) was used. C) The predicted peptide sequence after deleting the strand leading up to it in the MrkA protein sequence. This peptide sequence was added to the database, while still keeping the original sequence as well.

Discussion

In this study, we have characterized an amyloid fiber in *K. pneumoniae* isolate CA402 that contributes to the formation of a biofilm. Firstly, we determined which isolate to use for the experiments; of the seven isolates (KPN391, CA402, UTI3104, UTI4409, UTI4741, UTI5245 and UTI5829) CA402 showed to have the best results in case of biofilm formation on the side of the culture flasks as well as depiction of amyloid fibers in microscopy. The isolate showed a clear red line of biofilm, created at the air-liquid interface; biofilms formed at the air-liquid interface is also described in other bacteria, such as *Pseudomonas* and *Salmonella*, which are able to form biofilms ***(21, 22)***. Isolate CA402 was stained with CR, which is able to bind to amyloid fibers in biofilm forming pathogens. The brightfield- and fluorescence microscopy pictures of the biofilm, clearly illustrate a bundle of fibers with a threadlike structure, exhibiting a bright red color due to the CR stain. These findings indicate that the fibers in the biofilm are amyloid since CR binds to the β-backbone of amyloid fibers ***(15)***. However, CR staining is not a definitive factor for amyloid, therefore, EM was also performed to confirm our findings. TEM displayed these long, but aggregated, threadlike fibers, surrounding the bacteria, which fits the description of functional amyloids ***(15)***. Taking these findings into consideration: the formation of biofilm, presence of CR, and the structure of the fibers depicted by EM, we have amyloid fibers present in the biofilm created by *K. pneumoniae* isolate CA402.

The next step was to isolate the amyloid from the bacteria and biofilm, and thereafter digest the isolated amyloid protein to then later identify it. It is worth noting, we were only able to dissolve the amyloid protein from the biofilm by using formic acid prior to running SDS-PAGE, as formic acid is the only compound able to dissolve amyloids ***(15)***. In a study by Kimizuka et al., a CR-binding assay was used for identifying amyloid fibers in *Aggregatibacter actinomycetemcomitans* (*A. actinomycetemcomitans*) ***(23)***. They cultivated untreated *A. actinomycetemcomitans* on a CR agar plate, and *A. actinomycetemcomitans* pretreated with different proteolytics, as well as formic acid, on CR agar plates. They determined CR binding by resonance absorbance of the dye; the binding of CR was not affected in the untreated sample, nor in the pretreated samples with proteolytics. Yet, they showed that the binding of CR to *A. actinomycetemcomitans* was inhibited in the sample pretreated with formic acid; as formic acid disrupts the β-sheets in amyloids, they will not be able to bind CR. Thereby, Kimizuka et al. were able to confirm the presence of amyloid fibers in *A. actinomycetemcomitans*, by using CR and formic acid ***(23)***. This information supports our findings, that the distinctive band in the SDS-gel for the sample treated with formic acid, must be the band

containing the amyloid protein, since the protein can only be dissolved with high concentrations of formic acid.

After protein isolation and digestion was performed, MALDI and MS was subsequently performed. The spectrum displayed a few interesting peaks at 1510.783 m/z, 1713.786 m/z, 1870.937 m/z and 2239.158 m/z in the formic acid treated sample, which were different when compared to the peaks from the sample control. When further fragmenting and analyzing the peaks at 1713 m/z, 1870 m/z and 2239 m/z, no match with the protein sequences in the database was obtained. However, the peak at 1510 m/z seemed to be a lot more distinct from the control sample compared to the other identified peaks, and when further fragmenting and analyzing it with MS/MS, it matched with the MrkA protein in the database for CA402. With the help of a peptide prediction program, we were able to find a predicted signal peptide cleavage site on the protein sequence that our peptide fragment matched with. With this information, we removed the strand leading up to the cleavage point and then added the new peptide sequence into our CA402 database, to further improve our peptide match. After running MS/MS again, our peptide fragment aligned better with the new sequence in the database, providing us with a better match compared to the original sequence it had aligned with, which further supports the fact that this was a part of the MrkA protein. We then searched for the new predicted peptide sequence in the protein BLAST database, which gave several perfect matches with the known type 3 fimbria major subunit, MrkA, in *K. pneumoniae* strains. This confirmed our findings that the amyloid protein of *K. pneumoniae* is MrkA. In addition, amyloid fibers have a distinct cross-β backbone, which gives the fibers their helical appearance ***(15)***; this distinctive feature is also seen in the MrkA subunit of type 3 fimbriae, which has β-strands that contributes to its helical structure as well ***(10)***. Comparing this information to our findings, it further confirms that MrkA must be an amyloid fiber.

To our knowledge, no other studies have been conducted to characterize amyloid fibers in *K. pneumoniae* before, making it difficult to compare this study with other findings that would support ours. However, some studies have been conducted to illustrate the connection between type 3 fimbriae and biofilm formation in *K. pneumoniae*. A study by Schroll et al. shows that type 3 fimbriae in *K. pneumoniae* is essential for biofilm formation, compared to type 1 fimbriae ***(24)***. They compared a wild type strain, mutant strains that were either missing the type 1 or type 3 fimbriae gene cluster, and a mutant strain missing both. The wild type strain and the type 1 mutant had no difference in the ability of forming a biofilm. When comparing the wild type strain to the type 3 mutant and the type 1 and -3 mutant, the mutant strains only formed a very little amount of biofilm. Thus, they identified

that type 3 fimbria promotes the biofilm formation and therefore is essential for this process ***(24)***; this is also supported by other studies ***(25, 26)***. Another study by Langstraat et al. not only shows that type 3 fimbriae are responsible for biofilm formation, but that specifically the MrkA subunit and not the adhesive MrkD determined the formation of biofilm ***(27)***. They compared the ability of a wild type strain to form a biofilm onto the surface of microtiter plates to two mutant strains. The mutant strain lacking expression of MrkD was able to create a biofilm like the wild type strain, while the biofilm forming ability of the mutant strain, lacking expression of both MrkD and MrkA, was inhibited, meaning MrkA is essential for biofilm formation, but MrkD is not ***(27)***. Taking the findings from these studies into consideration, we can indirectly relate the importance of type 3 fimbriae and its MrkA subunit in biofilm formation, to our findings about MrkA of type 3 fimbriae being the amyloid fiber in *K. pneumoniae*.

Conclusion

Our aim of this study was to characterize a new *K. pneumoniae* amyloid fiber in biofilm formation. *K. pneumoniae* isolate CA402 was cultivated and stained with CR dye overnight, to then be examined by brightfield- and fluorescence microscopy. Due to the amyloid-specific dye CR, we were able to detect the formation of a biofilm and the presence of fibers in it, as CR colored the fibers red and when assessing the fibers in the fluorescence microscope, a red shift in light was observed, which is characteristic of amyloid fibers binding CR. Subsequent electron micrographs obtained by TEM identified the structure of the fibers surrounding the bacteria, illustrating they were long aggregated filaments, which is also characteristic of amyloids. From these findings, we are able to confirm that these fibers are amyloid fibers. We then treated the biofilm suspension with formic acid and isolated the assumed amyloid protein by SDS-PAGE. Subsequently, with the use of MALDI-TOF MS and MS/MS, we were able to identify the amyloid protein as the MrkA subunit of type 3 fimbriae in *K. pneumoniae*. With the information that the MrkA protein is the amyloid fiber responsible for the biofilm formation in *K. pneumoniae*, a better understanding is provided for the pathogenesis of this bacterium. With type 3 fimbriae on the surface of *K. pneumoniae*, we know the pathogen is able to form a biofilm on abiotic surfaces like urinary catheters. It would be interesting to investigate the ability of MrkA in *K. pneumoniae* to form biofilms on the surface of different materials. In this way, materials MrkA is not able to form a biofilm on, could be used for urinary catheters; thereby reducing the number of UTIs caused by catheters, since these cases are associated with biofilm formation.

Lastly, no one has characterized an amyloid fiber in a *K. pneumoniae* strain before, therefore, future studies are needed to further support our findings and confirming that MrkA is an amyloid fiber in *K. pneumoniae*.

References

1. Paczosa MK, Mecsas J (2016) Klebsiella pneumoniae: Going on the Offense with a Strong Defense. Microbiol Mol Biol Rev 80(3):629-661. 10.1128/MMBR.00078-15

2. Jensen TS, Opstrup KV, Christiansen G et al (2020) Complement mediated Klebsiella pneumoniae capsule changes. Microbes and infection 22(1):19-30. 10.1016/j.micinf.2019.08.003

3. Li B, Zhao Y, Liu C et al (2014) Molecular pathogenesis of Klebsiella pneumoniae. Future microbiology 9(9):1071-1081. 10.2217/fmb.14.48

4. Martin RM, Bachman MA (2018) Colonization, infection, and the accessory genome of Klebsiella pneumoniae. Frontiers in cellular and infection microbiology 8:4. 10.3389/fcimb.2018.00004

5. Clegg S, Murphy CN (2016) Epidemiology and Virulence of Klebsiella pneumoniae. Microbiology spectrum 4(1). 10.1128/microbiolspec.UTI-0005-2012

6. Shon AS, Bajwa RPS, Russo TA (2013) Hypervirulent (hypermucoviscous) Klebsiella pneumoniae. Virulence 4(2):107-118. 10.4161/viru.22718

7. Choby JE, Howard-anderson J, Weiss DS (2020) HypervirulentKlebsiella pneumoniae– clinical and molecular perspectives. J Intern Med 287(3):283. 10.1111/joim.13007

8. Agersø Y, Hald T, Helwigh B et al (2020) DANMAP 2011 - Use of antimicrobial agents and occurrence of antimicrobial resistance in bacteria from food animals, food and humans in Denmark. 10.13140/rg.2.2.32715.59680

9. Hansen SK, Kaya H, Roer L et al (2020) Molecular characterization of Danish ESBL/AmpC-producing Klebsiella pneumoniae from bloodstream infections, 2018. Journal of global antimicrobial resistance. 22:562-567. 10.1016/j.jgar.2020.05.014

10. Murphy CN, Clegg S (2012) Klebsiella pneumoniae and type 3 fimbriae: nosocomial infection, regulation and biofilm formation. Future microbiology 7(8):991-1002. 10.2217/fmb.12.74

11. Wilksch JJ, Yang J, Clements A et al (2011) MrkH, a novel c-di-GMP-dependent transcriptional activator, controls Klebsiella pneumoniae biofilm formation by regulating type 3 fimbriae expression. PLoS Pathogens 7(8):e1002204. 10.1371/journal.ppat.1002204

12. JOHNSON JG, CLEGG S (2010) Role of MrkJ, a Phosphodiesterase, in Type 3 Fimbrial Expression and Biofilm Formation in Klebsiella pneumoniae. Journal of Bacteriology 192(15):3944-3950. 10.1128/JB.00304-10

13. Johnson JG, Murphy CN, Sippy J et al (2011) Type 3 Fimbriae and Biofilm Formation Are Regulated by the Transcriptional Regulators MrkHI in Klebsiella pneumoniae. Journal of Bacteriology 193(14):3453-3460. 10.1128/JB.00286-11

14. Vestby LK, Grønseth T, Simm R et al (2020) Bacterial Biofilm and its Role in the Pathogenesis of Disease. Antibiotics 9(2):59. 10.3390/antibiotics9020059

15. Van Gerven N, Van der Verren, Sander E, Reiter DM et al (2018) The Role of Functional Amyloids in Bacterial Virulence. Journal of Molecular Biology 430(20):3657-3684. 10.1016/j.jmb.2018.07.010

16. Shewmaker F, McGlinchey RP, Wickner RB (2011) Structural Insights into Functional and Pathological Amyloid. The Journal of biological chemistry 286(19):16533-16540. 10.1074/jbc.R111.227108

17. Rambaran RN, Serpell LC (2008) Amyloid fibrils. Prion 2(3):112-117

18. Zhou Y, Blanco LP, Smith DR et al (2012) Bacterial Amyloids. In: Anonymous Amyloid Proteins, vol 849. Humana Press, Totowa, NJ, pp 303-320

19. Reichhardt C, Jacobson AN, Maher MC et al (2015) Congo red interactions with curli-producing E. coli and native curli amyloid fibers. PLoS ONE 10(10):e0140388. 10.1371/journal.pone.0140388

20. Shevchenko A, Mann M, Tomas H et al (2007) In-gel digestion for mass spectrometric characterization of proteins and proteomes. Nature protocols 1(6):2856-2860. 10.1038/nprot.2006.468

21. Jonas K, Tomenius H, Kader A et al (2007) Roles of curli, cellulose and BapA in Salmonella biofilm morphology studied by atomic force microscopy. BMC Microbiology 7(1):70. 10.1186/1471-2180-7-70

22. Dueholm MS, Søndergaard MT, Nilsson M et al (2013) Expression of Fap amyloids in P seudomonas aeruginosa , P . fluorescens, and P . putida results in aggregation and increased biofilm formation. MicrobiologyOpen 2(3):365. 10.1002/mbo3.81

23. Kimizuka R, Kato T, Hashimoto S et al (2009) Congo Red-binding Protein in Rough-phenotype Aggregatibacter actinomycetemcomitans is Amyloid-like Fiber. Bulletin of Tokyo Dental College 50(1):23-29. 10.2209/tdcpublication.50.23

24. Schroll C, Barken KB, Krogfelt KA et al (2010) Role of type 1 and type 3 fimbriae in Klebsiella pneumoniae biofilm formation. BMC microbiology 10(1):179. 10.1186/1471-2180-10-179

25. Martino PD, Cafferini N, Joly B et al (2003) Klebsiella pneumoniae type 3 pili facilitate adherence and biofilm formation on abiotic surfaces. Research in Microbiology 154(1):9. 10.1016/s0923-2508(02)00004-9

26. Burmølle M, Bahl MI, Jensen LB et al (2008) Type 3 fimbriae, encoded by the conjugative plasmid pOLA52, enhance biofilm formation and transfer frequencies in Enterobacteriaceae strains. Microbiology 154(1):187-195. 10.1099/mic.0.2007/010454-0

27. LANGSTRAAT J, BOHSE M, CLEGG S (2001) Type 3 Fimbrial Shaft (MrkA) of Klebsiella pneumoniae, but Not the Fimbrial Adhesin (MrkD), Facilitates Biofilm Formation. Infection and Immunity 69(9):5805-5812. 10.1128/IAI.69.9.5805-5812.2001